

Article

Microstructure and Mechanical Properties of Dissimilar Friction Welding Ti-6Al-4V Alloy to Nitinol

Ateekh Ur Rehman ^{1,*}, Nagumothu Kishore Babu ², Mahesh Kumar Talari ², Yusuf Siraj Usmani ¹ and Hisham Al-Khalefah ³

¹ Department of Industrial Engineering, College of Engineering, King Saud University, Riyadh 11421, Saudi Arabia; yusmani@ksu.edu.sa

² Department of Metallurgical and Materials Engineering, National Institute of Technology, Warangal 506004, India; kishorebabu@nitw.ac.in (N.K.B.); talari@nitw.ac.in (M.K.T.)

³ Advanced Manufacturing Institute, King Saud University, Riyadh 11421, Saudi Arabia; halkhalefah@ksu.edu.sa

* Correspondence: arehman@ksu.edu.sa

Abstract: In the present study, a friction welding process was adopted to join dissimilar alloys of Ti-6Al-4V to Nitinol. The effect of friction welding on the evolution of welded macro and microstructures and their hardnesses and tensile properties were studied and discussed in detail. The macrostructure of Ti-6Al-4V and Nitinol dissimilar joints revealed flash formation on the Ti-6Al-4V side due to a reduction in flow stress at high temperatures during friction welding. The optical microstructures revealed fine grains near the Ti-6Al-4V interface due to dynamic recrystallization and strain hardening effects. In contrast, the area nearer to the nitinol interface did not show any grain refinement. This study reveals that the formation of an intermetallic compound (Ti₂Ni) at the weld interface resulted in poor ultimate tensile strength (UTS) and elongation values. All tensile specimens failed at the weld interface due to the formation of intermetallic compounds.

Keywords: friction welding; Ti-6Al-4V; nitinol; intermetallic compound; fractography; dissimilar metal joining



Citation: Rehman, A.U.; Babu, N.K.; Talari, M.K.; Usmani, Y.S.; Al-Khalefah, H. Microstructure and Mechanical Properties of Dissimilar Friction Welding Ti-6Al-4V Alloy to Nitinol. *Metals* **2021**, *11*, 109. <https://doi.org/10.3390/met11010109>

Received: 9 December 2020

Accepted: 2 January 2021

Published: 7 January 2021

Publisher's Note: MDPI stays neutral with regard to jurisdictional claims in published maps and institutional affiliations.



Copyright: © 2021 by the authors. Licensee MDPI, Basel, Switzerland. This article is an open access article distributed under the terms and conditions of the Creative Commons Attribution (CC BY) license (<https://creativecommons.org/licenses/by/4.0/>).

1. Introduction

Titanium and titanium alloys are being widely used in several industrial applications because of their attractive properties, with a low density being one of them [1]. The most widely used $\alpha+\beta$ titanium alloy is Ti-6Al-4V (the workhorse grade in the titanium alloy group). This alloy finds extensive use in the medical industry and aerospace applications, due to its high specific strength, corrosion resistance, good fracture toughness, fatigue resistance, elevated temperature strength up to 500 °C, biocompatibility and weldability [1–4]. Nitinol, or titanium nickelide, belongs to the category of shape memory alloys, and it consists of an equiatomic alloy of nickel (Ni) and titanium (Ti). Nitinol is applied in the biomedical, aerospace, sensorics, fashion and automotive industries, as well as in structural elements and actuators, owing to its shape memory, biocompatibility and pseudoelasticity properties [5,6].

The joining of Ti-6Al-4V to Nitinol would be of great interest for many applications, including the hybrid welded structure of an adaptive gas turbine engine's toothed nozzle [7]. A joint made of Ti-6Al-4V joined to Nitinol adds the superelastic behavior of Nitinol to the excellent biocompatibility and corrosion resistance properties of these alloys. However, welding Ti-6Al-4V to Nitinol is challenging because of differences in their chemical and physical properties [8–10]. The functional behavior of NiTi alloys is strongly influenced by the chemical compositions and heat input of welding processes. Fusion welding readily forms stable intermetallic compounds (Ti₂Ni, Ni₃Ti) when titanium alloy is welded to Nitinol. The migration of Ni from Nitinol to the liquid titanium leads to the formation of

Ti₂Ni. These intermetallic compounds contribute to degradation of the mechanical properties of the welded joints [9–12]. These problems can be avoided by using an interlayer in between the Ti-Al-4V and Nitinol that inhibits or decreases the formation of intermetallic compounds in the weld zone [13].

NiTi was joined to another shape memory alloy, CuAlMn, by laser welding. A complex microstructure with islands of base metal deep inside the fusion zone were seen [14]. Datta et al. [15] did a feasibility study on the dissimilar joining of NiTi to Ti by laser welding. They reported that dissimilar welds exhibited poor strength and ductility due to the formation of Ti₂Ni phases and transverse cracks in the weld [15]. Similar problems occurred in Ti-6Al-4V-NiTiNb welds, too [9,16]. Though intermetallics in general reduce weld ductility in dissimilar metal combinations, some types of intermetallics seem to be less harmful. In NiTi-Cu laser welds, a larger Cu dilution means a greater amount of Cu-based intermetallics in the weld metal, and these Cu-based intermetallics prove beneficial for the weld ductility when compared to Ti-based intermetallics [17,18].

The problem of brittle phases was overcome by placing an Nb interlayer with a thickness of 50 µm in between the Ti-6Al-4V and NiTi in laser welding [19]. The interlayer acted as a diffusion barrier between the two base metals. By varying the laser power and thereby controlling the Nb dilution, Zhou et al. could control the overall amount of intermetallics within the weld [20]. When the Nb melted completely, the joint strength shot up to as high as 82% of the Ti-6Al-4V base metal strength. Even electron beam welding produced similar effects [21].

Another possibility is to explore the solid state welding process to join Ti-Al-4V to Nitinol, in which the joining of materials takes place without melting and without the use of any filler. Solid state welding, like friction welding, can alleviate to some extent the fusion welding problems described above. Friction welding is a solid state welding process in which joining is achieved by one placing work piece in the rotating fixture and the other in a stationary fixture, and frictional heat is generated by the pressure and relative motion between these work pieces. Senkevich et al. [22] studied the joints of Ti-54.2% Ni with VT6 titanium alloy by the diffusion bonding technique. They observed a transition zone between the connected alloys, and this zone exhibited a higher hardness compared with the two base metals due to enrichment of the titanium. It was reported that a maximum shear strength of 170 MPa was achieved at 950 °C and a 30 min holding time. Wei Zhang et al. [23] investigated the microstructure and mechanical properties of Nitinol-Nitinol joints by ultrasonic welding, using Cu as an interlayer. They found that no intermetallic layer was observed at the joint interface. It was reported that the ultimate shear load increased with the increasing weld energy from 500 J to 1000 J due to metallurgical bonding at the interface.

There were quite a few successful attempts at joining Nitinol to Nitinol, whether it was through fusion welding [24,25] or solid-state welding [26,27]. However, when it came to joining Nitinol to Ti-Al-4V, the reports were few and far between, and even then, the welds turned out to be substantially poor in quality. All these published works dealt with fusion welding only [9–21]. This knowledge gap threw open the opportunity for us to attempt the same weld combination through a solid state joining technique like friction welding. Friction welding had already proved itself as a promising technique in several other dissimilar metal combinations. To the authors' best knowledge, this is one of the first attempts at joining Nitinol to Ti-Al-4V. This study demonstrates how, by choosing weld parameters carefully, we could obtain significantly strong welds between Nitinol and Ti-Al-4V. At the same time, some of the challenges that still need to be overcome before this promising combination of dissimilar metals could be used in wide-ranging applications have been identified.

2. Materials and Methods

Ti-6Al-4V and Nitinol rods 100 mm in length with a cross-sectional diameter of 10 mm were used in the present investigation. The chemical compositions of these alloys are

listed in Table 1. The rods of Ti-6Al-4V and Nitinol alloys were face turned and cleaned with acetone before friction welding. Continuous drive friction welding with a capacity of 150 kN was employed for the friction welding of dissimilar materials (Figure 1). Ti-6Al-4V was held in the non-rotating vice and Nitinol in the rotating chuck. At the start of the friction welding process, the rotating spindle quickly reached a set speed (spindle speed). The non-rotating specimen was then pushed toward the rotating one under high pressure (friction pressure). Due to the relative motion between the two specimens under pressure, frictional heat was generated at the interface. This heat very quickly plasticized both of the base metals, resulting in a flash. The flash, in fact, helps by ejecting out impurities and oxide layers from the surface of the specimens. The loss in the overall length of the rods was monitored by a sensor, and when the set burn-off length was achieved, the rotating chuck was suddenly brought to rest using a brake. This ended the first stage of the weld cycle, called the friction stage. In the next stage (the upset stage), the pressure was further increased (upset pressure) and held constant for a certain length of time (upset time). The bond consolidation between the two specimens was thus completed.

Table 1. Composition of base metals (wt%).

Elements	Al	V	Fe	Cr	C	N	O	H	Ti
Ti-6Al-4V	6.01	4.0	0.04	0.14	0.01	0.004	0.114	0.008	balance
Elements	Ni	Co	Cr	Fe	Nb	C	O	H	Ti
Nitinol	55.7	0.005	0.003	0.015	0.005	0.04	0.036	<0.001	balance

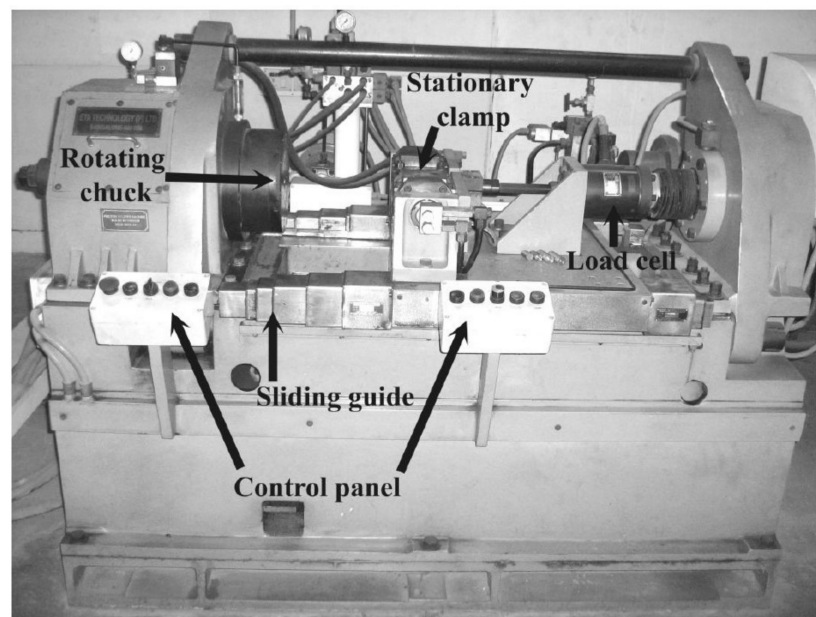


Figure 1. Friction welding machine used in the current study.

The initial parameter window considered is listed in Table 2. At first, one parameter was varied at a time to see how it affected the quality of the welds. Here, quality was assessed by two simple and quick methods: visual inspection of the flash and how the welds survived a drop test. The upset pressure, spindle speed and upset time did not have a significant effect, whereas the friction pressure and burn-off length noticeably influenced the weld quality. In the second stage, just these parameters (friction pressure and burn-off length) were changed by two levels each. Again, based on visual inspection, a final set of parameters was selected, and the same set was used for all the subsequent welds in the current work (Table 2).

Table 2. Welding parameters.

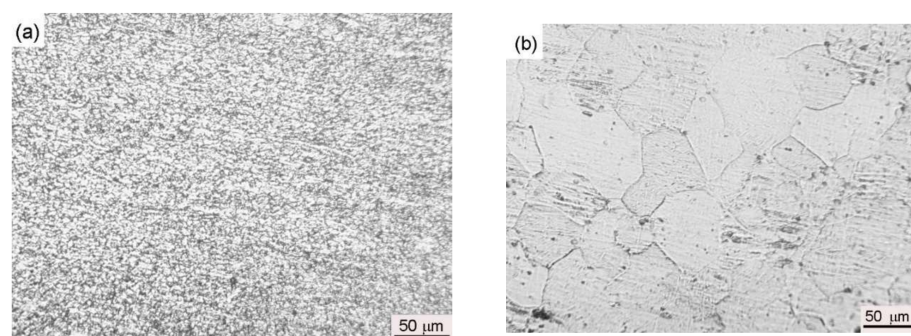
	Explored Parameter Range	Final Parameters Chosen
Friction Pressure	50–250 MPa	60 MPa
Upset Pressure	100–400 MPa	150 MPa
Spindle Speed	1000–2000 rev/min	1400 rev/min
Burn-off Length	1–7 mm	5 mm
Upset Time	4–10 s	5 s

A solution containing 2% HF and 3% HNO₃ in 95% distilled water was used to etch the Ti-6Al-4V alloy weld, and 40% HNO₃ and 10% HF in 50% distilled water was used to etch the Nitinol weld. The chemical compositions of the Ti-6Al-4V alloy to the Nitinol rods were analyzed by employing a LECO TCH 400 instrument (LECO Corporation, St. Joseph, MI, USA). The low-magnification macrostructure of the friction welds was observed using a Nikon SMZ745T stereo microscope (Nikon Instruments Inc., New York, NY, USA). The microstructural features of the friction welded samples were observed using a Leitz optical microscope. The microstructure and energy dispersive spectroscopy (EDS) line scan were investigated using a VEGA 3LMV, TESCAN scanning electron microscope and oxford instruments, respectively (TESCAN ORSAY HOLDING, Brno, Czech Republic). X-ray diffraction (XRD) analysis (PANalytical, Malvern, UK, X'pert powder XRD) was used to identify phases in the base metal and weld. Vickers microhardness measurements were carried out as per the ASTM E384 standard (West Conshohocken, PA, USA) across the weld region by using a diamond pyramid indenter under a load of 500 g for 15 s (MMT-X Matsuzawa, Akita Prefecture, Kawabetoshima, Japan). Transverse weld specimens of a 25 mm gauge length and 4 mm diameter were machined from friction welded samples. Tensile tests were carried out according to the ASTM E8 standard on the base metal, as well as dissimilar friction welded samples using a servo hydraulic testing machine at a constant displacement rate of 0.5 mm/min.

3. Results and Discussion

3.1. Base Metal Microstructures

The optical microstructures of the Ti-6Al-4V and Nitinol alloys are shown in Figure 2a,b respectively. Both microstructures showed equiaxed grains, and the average grain sizes of the Ti-6Al-4V and the Nitinol were $7 \pm 1 \mu\text{m}$ and $50 \pm 8 \mu\text{m}$, respectively. The optical microstructure of the Ti-6Al-4V revealed alpha grains (brighter phase) in a transformed beta matrix (darker phase). Predominantly, a single-phase equiaxed microstructure was seen, with distinct twin lines in the Nitinol. Nitinol transforms to an austenitic phase when heated to a point above its austenite start (A_s) temperatures, but reverts back to its stable state of a martensitic phase when cooled [5]. Depending on the Ni content, the start and finish temperatures of the phase transformation varies. However, it is safe to assume that the present alloy remained predominantly austenitic at room temperature, with possible tiny volumes of a martensitic phase.

**Figure 2.** Optical microstructures of the base metals (a) Ti-6Al-4V and (b) Nitinol.

3.2. Macro and Microstructures of Dissimilar Friction Welds

An actual Ti-6Al-4V and Nitinol joint is shown in Figure 3. Visual examination revealed no obvious macroscopic defects. The low-magnification friction welded joint made between the Ti-6Al-4V and Nitinol alloys showed a flash formation, which is a typical characteristic of the friction welding process (Figure 3). The flash predominantly occurred on the Ti-6Al-4V side, but for the Nitinol it was notably absent. From Figure 4, it is worthwhile to note that a precipitous drop in flow stresses in Ti-6Al-4V at high temperatures during friction welding makes the alloy softer compared with the Nitinol side, even though the yield strength (YS) of Ti-6Al-4V is higher than Nitinol to begin with at room temperature [28]. In addition to this, the poor heat conducting properties of Ti-6Al-4V cause the temperature to rise quickly on its side of the joint.



Figure 3. The visual view of a Ti-6Al-4V and Nitinol dissimilar friction welded joint.

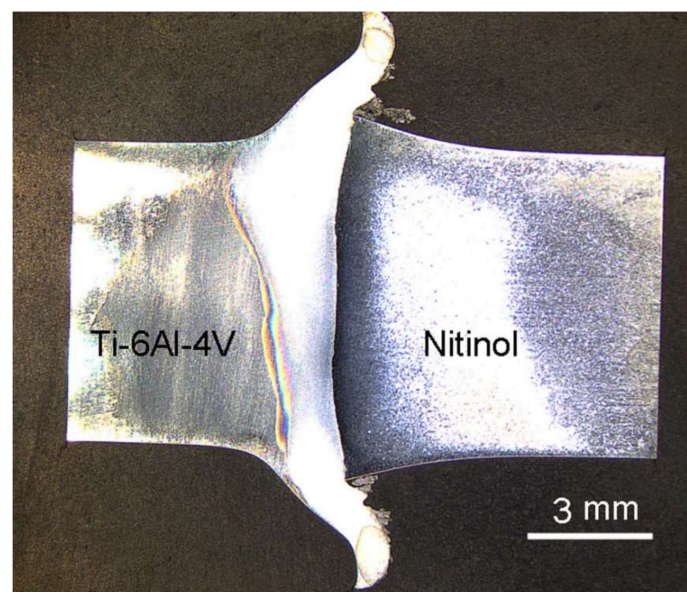


Figure 4. Dissimilar friction welded Ti-6Al-4V and Nitinol sample showing the flash on the Ti-6Al-4V side.

The optical microstructure of the Ti-6Al-4V/Nitinol joint interface is shown in Figure 5a. The grains nearer to the interface on the Ti-6Al-4V side underwent refinement, whereas the Nitinol microstructure largely remained unaffected. Friction welding introduced a lot of dislocations into the materials because of the heavy plastic deformation that occurred during the process and, at the same time, it generated high temperatures close to the melting point of the base metals. The subgrain structure could also be seen if the dislocation density increased. These low-angle grain boundaries rotated to form stain-free grains, which are fine grains referred to as dynamic recrystallization (DRX) [29]. DRX was observed on

the Ti-6Al-4V side, adjacent to the joint interface when compared with the Nitinol side. This means that the deformation was more on the Ti-6Al-4V side due to the heavy plastic deformation and high temperatures encountered in friction welding. Due to dynamic recrystallization, nucleation and growth of the grains occurred; hence, a large amount of fine equiaxed grains were observed adjacent to the Ti-6Al-4V interface. A darker region (intermixed zone) was noticed between the Ti-6Al-4V/Nitinol joint interface. This may be due to the formation of intermetallics at the interface. The grains along the Ti-6Al-4V interface aligned in the rotating direction due to deformation of the material, as shown in Figure 5 b. The dark spots observed on the welded samples were referred to as etch pits, developed during etching of the sample. There was no significant change in grain size adjacent to the Nitinol interface, and the microstructure consisted mainly of austenite rather than martensite due to the heating of the material during welding.

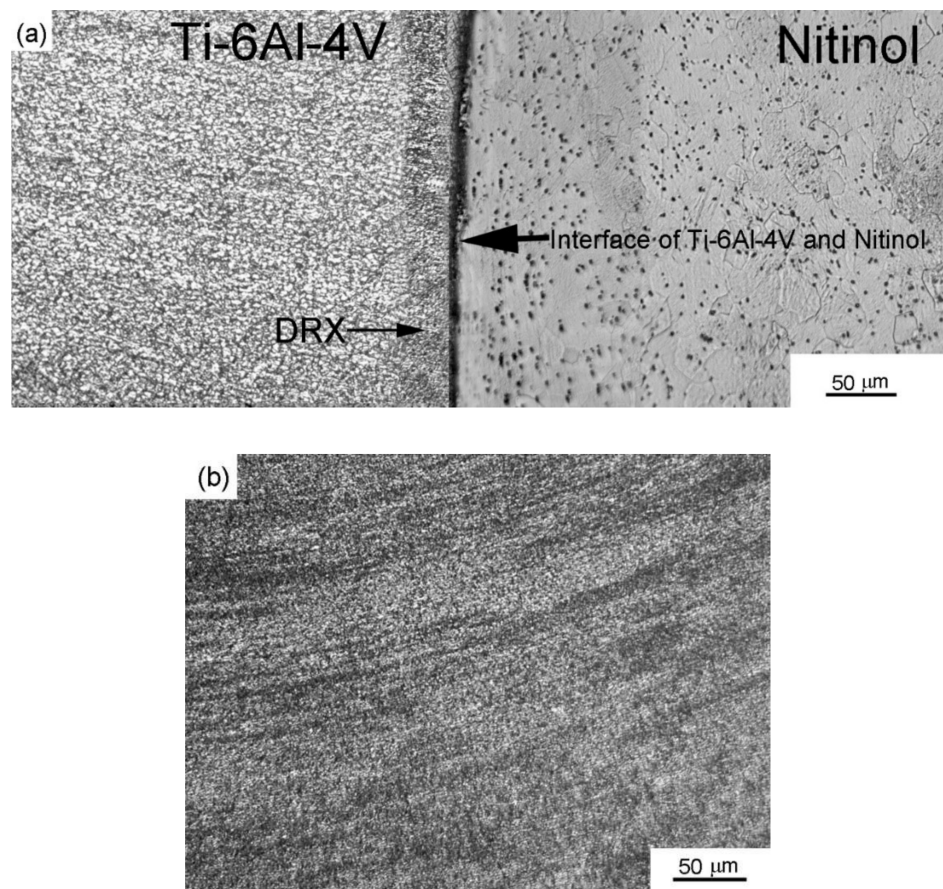


Figure 5. (a) The optical microstructure of the Ti-6Al-4V/Nitinol joint interface. (b) The grains along the titanium interface, aligned in the rotating direction.

Figure 6 shows a scanning electron microscopy (SEM) image of the Ti-6Al-4V/Nitinol joint and the corresponding SEM EDS line scan, which shows the distribution of different elements across the joint. The EDS line scan revealed an interface between the Ti-6Al-4V/Nitinol joint, and here, a ~10 μm wide intermixed zone could be seen. The intermixed zone was the result of the huge amount of plastic strains and high temperatures seen in this region. It is also reasonable to expect that this intermixed zone would not be of the same width and composition between the center and the periphery [30]. This is because the intensity of rubbing differs in these zones. Ni has low solubility in Ti in its solid state and forms the brittle intermetallic compound Ti_2Ni . These hard intermetallic compounds play a major role in the poor ductility of Ti-6Al-4V/Nitinol welds [9–12]. It is worth noting that even though the initial diffusion rates depend upon the alloying elements present in each of the base metals, the newly formed intermetallic phases would also start to influence

the diffusion phenomenon very quickly [30]. There is also the possibility of formation of Kirkendall voids when a particular element undergoes mass transport while it forms the reaction products in dissimilar material joining [31].

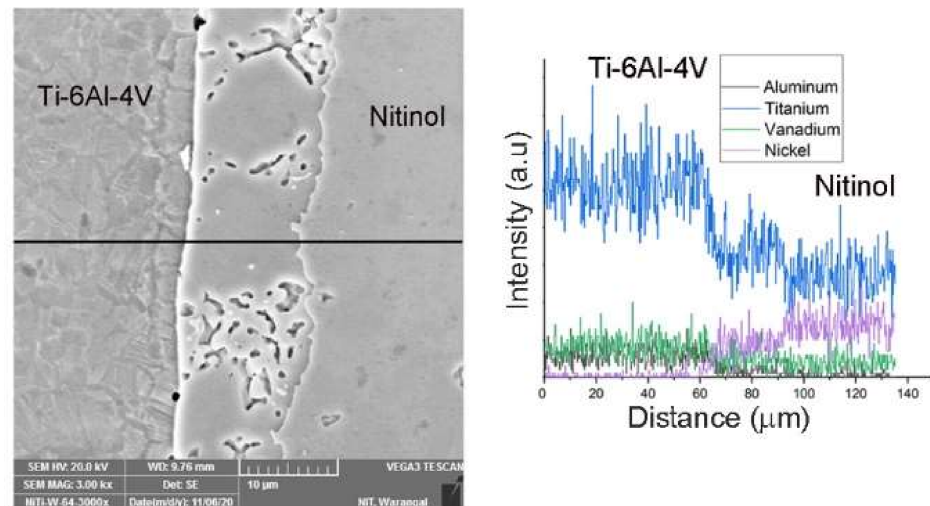


Figure 6. SEM image of the Ti-6Al-4V/Nitinol joint and the corresponding SEM energy dispersive spectroscopy (EDS) line scan.

The diffusion of Ni into Ti-6Al-4V was relatively higher. Figure 7 shows the X-ray diffraction analysis of the Ti-6Al-4V base metal, Nitinol base metal and fracture surface of the weld. The Nitinol base metal exhibited a B2 austenitic phase, and the Ti-6Al-4V base metal exhibited a hexagonal α phase and a weak β phase. In contrast, the fracture surface of the weld revealed a hexagonal α phase, β phase and the formation of a Ti_2Ni brittle intermetallic phase.

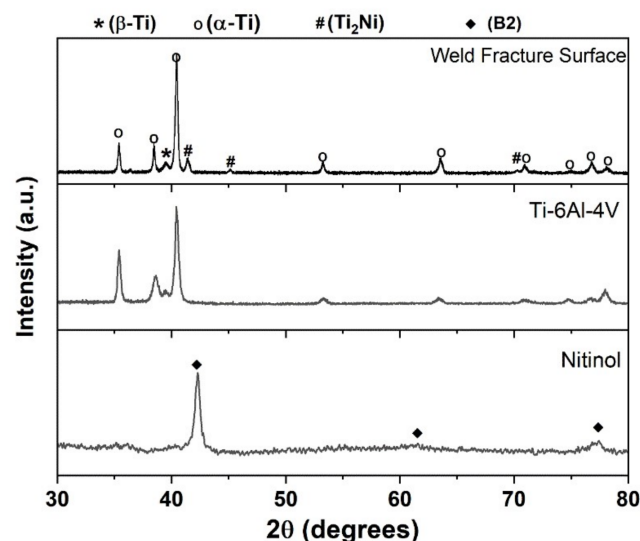


Figure 7. X-ray diffraction (XRD) profiles of the Ti-6Al-4V base metal, Nitinol base metal and fracture surface of the Ti-6Al-4V/Nitinol friction welds.

3.3. Mechanical Properties

3.3.1. Hardness

Figure 8 shows the hardness distribution across the interfaces of dissimilar Ti-6Al-4V/Nitinol welds. It is observed that there was an increase in hardness on the Ti-6Al-4V side due to strain hardening that occurred during the friction welding process. However, no significant increase in hardness is observed on the Nitinol side, which confirms the previous

observation that there was no significant deformation on the Nitinol side. Similar results were observed in previous studies involving friction welding of commercially pure Ti to 304L stainless steel [28,32]. Dissimilar friction welds prepared from Ti to 304L stainless steel have shown an increase in hardness on the Ti side due to the strain hardening effect when compared with the stainless steel side. However, a decrease in hardness on the stainless steel side was attributed to a limited amount of deformation or the lack of a strain hardening effect [28]. The Ti-6Al-4V and Nitinol base materials had average hardnesses of 367 ± 18 HV and 260 ± 16 HV, respectively. The highest hardness observed at the Ti-6Al-4V/Nitinol interface may be attributed to the formation of intermetallics of Ti and Ni, such as Ti_2Ni , a result conformed by XRD analysis.

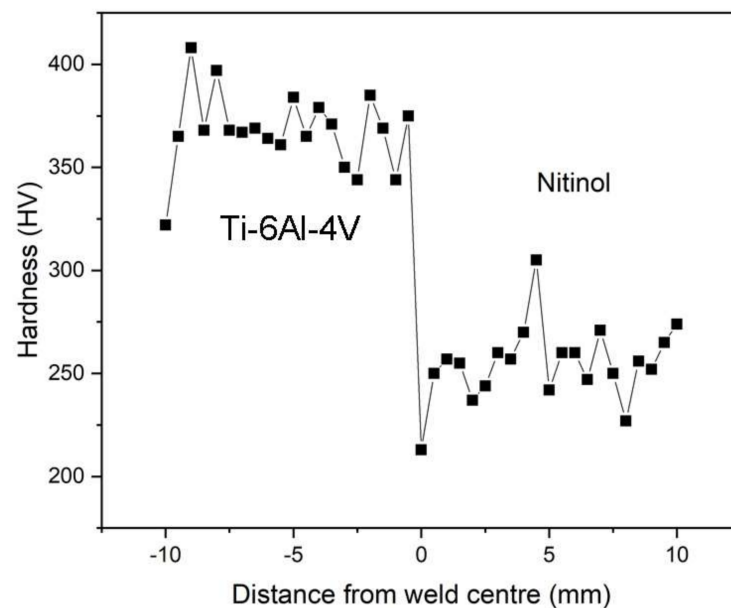


Figure 8. The hardness distribution across the interface of dissimilar Ti-6Al-4V/Nitinol welds.

3.3.2. Tensile Properties

The tensile properties of dissimilar Ti-6Al-4V/Nitinol friction welds are shown in Figure 9. The important objective of the present investigation was to determine whether the joint strength of a dissimilar weld shows any improvement in its weld zone tensile properties. The data of two base materials' tensile properties have also been included in Figure 8 for comparison. It is revealed from Figure 9 that the dissimilar Ti-6Al-4V/Nitinol friction weld exhibited a lower ultimate tensile strength (UTS) and ductility (UTS = 589 MPa, 3.9% elongation) compared with the base metals (Ti-6Al-4V: UTS = 1073 MPa, 15% elongation; Nitinol: UTS = 980 MPa, 16% elongation). This could be because of intermetallic formations (Ti_2Ni) at the interface which are brittle in nature. Similar results were observed in laser welding of dissimilar Ti-6Al-4V to NiTi joints [10]. These dissimilar welds exhibited a UTS value of 250 MPa and 3% elongation. The authors attributed the reason for the inferior properties to the formation of a Ti_2Ni phase and transverse cracks in the weld metal. Electron beam welding was better in that the UTS was 480 MPa with 2.3% elongation [21]. Three tensile tests were conducted for each condition, and the average of these specimens was taken. The dissimilar weld failed in the intermixed zone, except for the Ti-6Al-4V and Nitinol base metals. Failure in the intermixed zone indicates that the weld region was weaker than the base metals in the dissimilar welded joint. The tensile fracture surfaces of the Ti-6Al-4V base metal, Nitinol base metal and dissimilar Ti-6Al-4V/Nitinol friction welds are shown in Figure 10. Very fine and ductile fracture features were observed for the Ti-6Al-4V and Nitinol base metals in Figure 10a,b respectively. It is well established that the fine equiaxed dimples are observed in the base metal samples because of microvoid

formation and joining. Figure 10c shows the cleavage fracture (brittle) features of dissimilar Ti-6Al-4V/Nitinol friction welds.

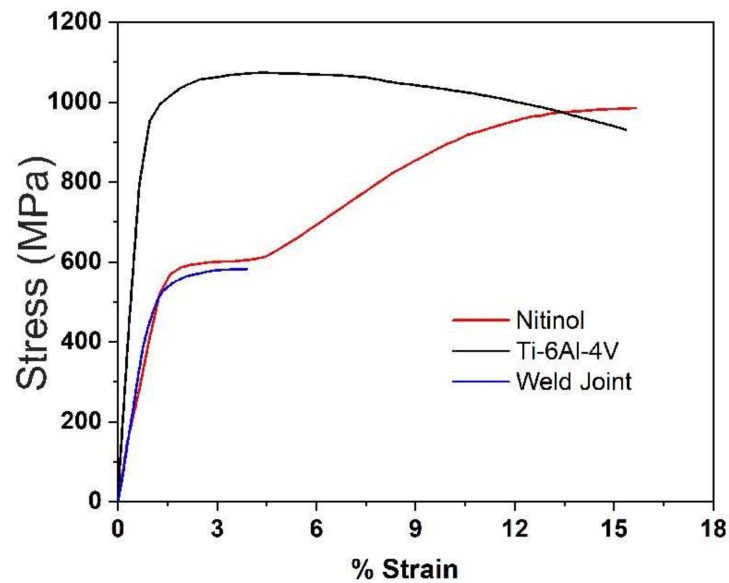


Figure 9. The tensile properties of base metals and dissimilar Ti-6Al-4V/Nitinol friction welds.

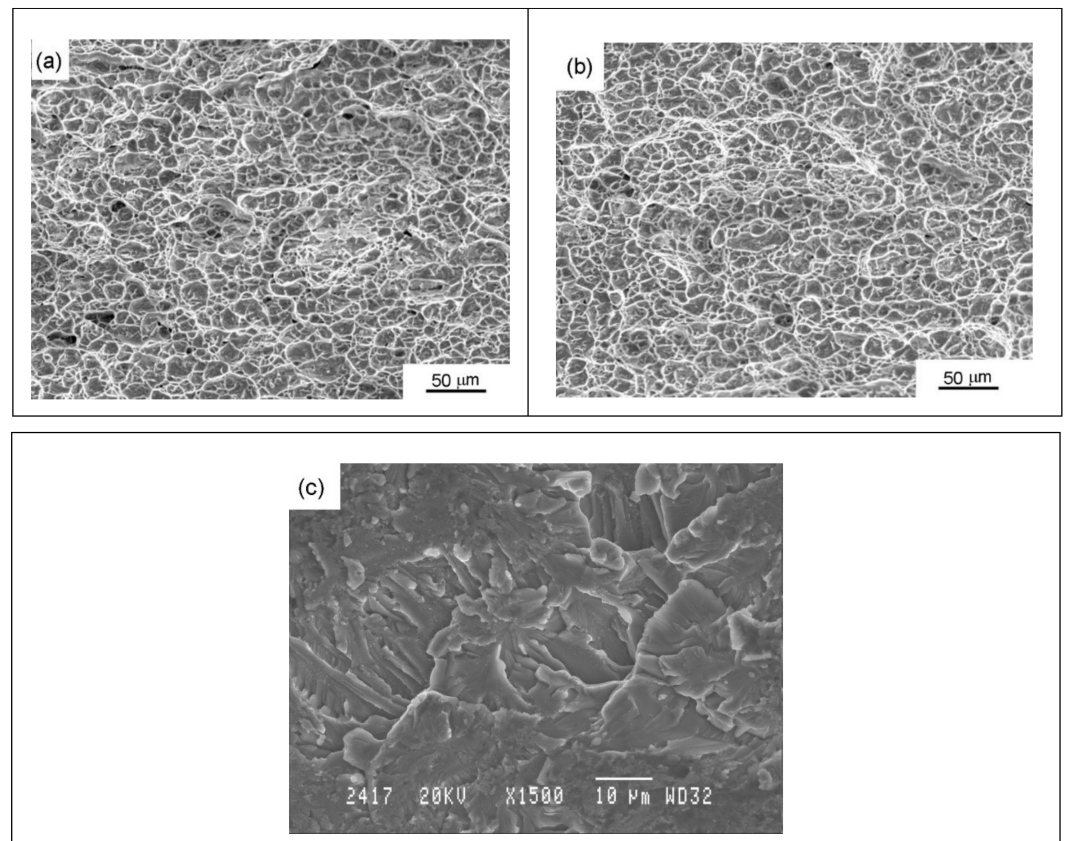


Figure 10. Fracture surfaces of the base metals and dissimilar welded joint for (a) Ti-6Al-4V, (b) Nitinol and (c) dissimilar Ti-6Al-4V/Nitinol friction welded joint.

4. Conclusions

Dissimilar Ti-6Al-4V/Nitinol friction welds have been analyzed for weld macro and microstructures, grain sizes, hardnesses and tensile properties. The following conclusions can be drawn:

1. A defect-free dissimilar friction weld could be obtained by a continuous drive friction welding machine;
2. The macrostructure of dissimilar Ti-6Al-4V/Nitinol friction welds revealed flash formation only on the Ti-6Al-4V side due to the reduction in flow stress at high temperatures experienced during friction welding;
3. XRD studies revealed the formation of an intermetallic compound (Ti_2Ni) on the fracture surface of dissimilar welds;
4. The dissimilar Ti-6Al-4V/Nitinol friction weld exhibited low strength and ductility (UTS = 589 MPa, 3.9% elongation) compared with the base metals, and this may be attributed to the formation of Ti_2Ni intermetallics at the interface, which are brittle in nature;
5. The tensile fracture surfaces observed in dissimilar Ti-6Al-4V/Nitinol friction welds had cleavage (brittle) fracture features due to the formation of intermetallics at the intermixed zone when compared with the fine dimples noticed in the base metal samples.

Author Contributions: Conceptualization, A.U.R., Y.S.U. and H.A.-K.; methodology, A.U.R., N.K.B., M.K.T. and Y.S.U.; formal analysis, A.U.R., N.K.B., M.K.T., Y.S.U. and H.A.-K.; investigation, A.U.R., N.K.B., M.K.T. and Y.S.U.; resources, A.U.R., Y.S.U. and H.A.-K.; data curation, A.U.R., N.K.B. and M.K.T.; writing—original draft preparation, A.U.R., N.K.B. and M.K.T.; writing—review and editing, A.U.R., N.K.B., M.K.T., Y.S.U. and H.A.-K.; visualization, A.U.R., N.K.B. and M.K.T.; supervision, A.U.R., N.K.B. and M.K.T.; project administration, A.U.R., and Y.S.U.; funding acquisition, A.U.R., Y.S.U. and H.A.-K. All authors have read and agreed to the published version of the manuscript.

Funding: This research was funded by the National Plan for Science, Technology and Innovation (MAARIFAH), King Abdulaziz City for Science and Technology, Kingdom of Saudi Arabia, Award Number (14-ADV110-02).

Institutional Review Board Statement: Not applicable.

Informed Consent Statement: Not applicable.

Data Availability Statement: Data is contained within the article “Microstructure and Mechanical Properties of Dissimilar Friction Welded Ti-6Al-4V to Nitinol Joints”.

Acknowledgments: This Project was funded by the National Plan for Science, Technology and Innovation (MAARIFAH), King Abdulaziz City for Science and Technology, Kingdom of Saudi Arabia, Award Number (14-ADV110-02). The authors acknowledge Ashfaq Mohammad at the National Manufacturing Institute Scotland for his technical inputs during the experimental and writeup stages of the present work.

Conflicts of Interest: The authors declare no conflict of interest.

References

1. Boyen, R.R. Titanium and titanium alloys. In *Metals Handbook*; Davis, J.R., Ed.; ASM International: Materials Park, OH, USA, 1998; pp. 575–588. ISBN 978-0-87170-654-6.
2. Sidambe, A. Biocompatibility of Advanced Manufactured Titanium Implants—A Review. *Materials* **2014**, *7*, 8168–8188. [[CrossRef](#)] [[PubMed](#)]
3. Niinomi, M. Mechanical properties of biomedical titanium alloys. *Mater. Sci. Eng. A* **1998**, *243*, 231–236. [[CrossRef](#)]
4. Gurrappa, I. Characterization of titanium alloy Ti-6Al-4V for chemical, marine and industrial applications. *Mater. Charact.* **2003**, *51*, 131–139. [[CrossRef](#)]
5. Jani, J.M.; Leary, M.; Subic, A.; Gibson, M.A. A Review of Shape Memory Alloy Research, Applications and Opportunities. *Mater. Des.* **2013**. [[CrossRef](#)]
6. Saedi, S.; Turabi, A.S.; Andani, M.T.; Moghaddam, N.S.; Elahinia, M.; Karaca, H.E. Texture, aging, and superelasticity of selective laser melting fabricated Ni-rich NiTi alloys. *Mater. Sci. Eng. A* **2017**, *686*, 1–10. [[CrossRef](#)]

7. Chau, E.T.F. Comparative Study of Joining Methods for a SMART Aerospace Application. Ph.D. Thesis, Cranfield University, Cranfield, UK, 2007.
8. Sun, Z.; Ion, J.C. Laser welding of dissimilar metal combinations. *J. Mater. Sci.* **1995**, *30*, 4205–4214. [[CrossRef](#)]
9. Miranda, R.M.; Assunção, E.; Silva, R.J.C.; Oliveira, J.P.; Quintino, L. Fiber laser welding of NiTi to Ti-6Al-4V. *Int. J. Adv. Manuf. Technol.* **2015**, *81*, 1533–1538. [[CrossRef](#)]
10. Shojaei Zoeram, A.; Akbari Mousavi, S.A.A. Laser welding of Ti-6Al-4V to Nitinol. *Mater. Des.* **2014**, *61*, 185–190. [[CrossRef](#)]
11. Falvo, A.; Furguele, F.M.; Maletta, C. Functional behaviour of a NiTi-welded joint: Two-way shape memory effect. *Mater. Sci. Eng. A* **2008**, *481*, 647–650. [[CrossRef](#)]
12. Otsuka, K.; Wayman, C.M. (Eds.) *Shape Memory Materials*, 1st ed.; Cambridge Univ. Press: Cambridge, UK, 1999; ISBN 978-0-521-44487-3.
13. Oliveira, J.P.; Miranda, R.M.; Braz Fernandes, F.M. Welding and Joining of NiTi Shape Memory Alloys: A Review. *Prog. Mater. Sci.* **2017**, *88*, 412–466. [[CrossRef](#)]
14. Oliveira, J.P.; Zeng, Z.; Andrei, C.; Braz Fernandes, F.M.; Miranda, R.M.; Ramirez, A.J.; Omori, T.; Zhou, N. Dissimilar laser welding of superelastic NiTi and CuAlMn shape memory alloys. *Mater. Des.* **2017**, *128*, 166–175. [[CrossRef](#)]
15. Datta, S.; Raza, M.S.; Kumar, S.; Saha, P. Exploring the possibility of dissimilar welding of NiTi to Ti using Yb-fiber laser. *Adv. Mater. Process. Technol.* **2018**, *4*, 614–625. [[CrossRef](#)]
16. Yuhua, C.; Yuqing, M.; Weiwei, L.; Peng, H. Investigation of welding crack in micro laser welded NiTiNb shape memory alloy and Ti6Al4V alloy dissimilar metals joint. *Opt. Laser Technol.* **2017**, *91*, 197–202. [[CrossRef](#)]
17. Zeng, Z.; Panton, B.; Oliveira, J.P.; Han, A.; Zhou, Y.N. Dissimilar laser welding of NiTi shape memory alloy and copper. *Smart Mater. Struct.* **2015**, *24*, 1–8. [[CrossRef](#)]
18. Zeng, Z.; Oliveira, J.P.; Yang, M.; Song, D.; Peng, B. Functional fatigue behavior of NiTi-Cu dissimilar laser welds. *Mater. Des.* **2017**, *114*, 282–287. [[CrossRef](#)]
19. Oliveira, J.P.; Panton, B.; Zeng, Z.; Andrei, C.M.; Zhou, Y.; Miranda, R.M.; Braz Fernandes, F.M. Laser joining of NiTi to Ti6Al4V using a Niobium interlayer. *Acta Mater.* **2016**, *105*, 9–15. [[CrossRef](#)]
20. Zhou, X.; Chen, Y.; Huang, Y.; Mao, Y.; Yu, Y. Effects of niobium addition on the microstructure and mechanical properties of laser-welded joints of NiTiNb and Ti6Al4V alloy. *J. Alloys Compounds* **2018**, *735*, 2616–2624. [[CrossRef](#)]
21. Zhan, Z.; Chen, Y.; Wang, S.; Huang, Y.; Mao, Y. Prevention of crack formation in electron-beam welded joints of dissimilar metal compounds (TiNi/Ti-6Al-4V). *Metal Sci. Heat Treat.* **2019**, *61*, 373–378. [[CrossRef](#)]
22. Senkevich, K.S.; Knyazev, M.I.; Runova, Y.E.; Shlyapin, S.D. Special Features of Formation of a TiNi-VT6 Diffusion Joint. *Met. Sci. Heat Treat.* **2013**, *55*, 419–422. [[CrossRef](#)]
23. Zhang, W.; Ao, S.; Oliveira, J.; Zeng, Z.; Huang, Y.; Luo, Z. Microstructural Characterization and Mechanical Behavior of NiTi Shape Memory Alloys Ultrasonic Joints Using Cu Interlayer. *Materials* **2018**, *11*, 1830. [[CrossRef](#)]
24. Gugel, H.; Schuermann, A.; Theisen, W. Laser welding of NiTi wires. *Mater. Sci. Eng. A* **2008**, *481*, 668–671. [[CrossRef](#)]
25. Yang, D.; Jiang, H.C.; Zhao, M.J.; Rong, L.J. Microstructure and mechanical behaviors of electron beam welded NiTi shape memory alloys. *Mater. Des.* **2014**, *57*, 21–25. [[CrossRef](#)]
26. London, B.; Fino, J.; Pelton, A.R.; Mahoney, M. Friction stir processing of Nitinol. In Proceedings of the Friction Stir Welding and Processing III, TMS Annual Meeting, San Francisco, CA, USA, 13–17 February 2005; Jata, K.V., Mahoney, M.W., Mishra, R.S., Lienert, T.J., Eds.; TMS (The Minerals, Metals and Materials Society): San Francisco, CA, USA, 2005; pp. 67–74.
27. Shinoda, T.; Tsuchiya, T.; Takahashi, H. Friction welding of shape memory alloy. *Weld. Int.* **1992**, *6*, 20–25. [[CrossRef](#)]
28. Muralimohan, C.H.; Muthupandi, V.; Sivaprasad, K. Properties of Friction Welding Titanium-stainless Steel Joints with a Nickel Interlayer. *Procedia Mater. Sci.* **2014**, *5*, 1120–1129. [[CrossRef](#)]
29. Mishra, R.S.; Ma, Z.Y. Friction stir welding and processing. *Mater. Sci. Eng. R Rep.* **2005**, *50*, 1–78. [[CrossRef](#)]
30. Zhang, Y.; Sun, D.Q.; Gu, X.Y.; Li, H.M. Nd:YAG pulsed laser welding of dissimilar metals of titanium alloy to stainless steel. *Int. J. Adv. Manuf. Technol.* **2018**, *94*, 1073–1085. [[CrossRef](#)]
31. Wang, Y.; Prangnell, P.B. The significance of intermetallic compounds formed during interdiffusion in aluminum and magnesium dissimilar welds. *Mater. Charact.* **2017**, *134*, 84–95. [[CrossRef](#)]
32. Dey, H.C.; Ashfaq, M.; Bhaduri, A.K.; Rao, K.P. Joining of titanium to 304L stainless steel by friction welding. *J. Mater. Process. Technol.* **2009**, *209*, 5862–5870. [[CrossRef](#)]